A STUDY OF CONSTANT ABSOLUTE VORTICITY TRAJECTORIES ON ISENTROPIC SURFACES

E. M. CARLSTEAD

Add to Shopping Cart | Save for Later

Technical Reports Collection

Citation Format: Full Citation (1F)

Accession Number :
AD0480921
Citation Status:
Active
Citation Classification:
Unclassified
SBI Site Holding Symbol:
AWS/TECH
Field(s) & Group(s):
040200 - METEOROLOGY
200400 - FLUID MECHANICS
Corporate Author:
NAVAL POSTGRADUATE SCHOOL MONTEREY CA
Unclassified Title:
A STUDY OF CONSTANT ABSOLUTE VORTICITY TRAJECTORIES ON ISENTROPIC SURFACES.
Title Classification:
Unclassified
Descriptive Note:
Master's thesis,
Personal Author(s):

Add to Shopping Cart | Save for Later

Technical Reports Collection

Citation Format: Full Citation (1F)

Accession Number :
AD0480921
Citation Status:
Active
Citation Classification:
Unclassified
SBI Site Holding Symbol:
AWS/TECH
Field(s) & Group(s):
040200 - METEOROLOGY
200400 - FLUID MECHANICS
Corporate Author:
NAVAL POSTGRADUATE SCHOOL MONTEREY CA
Unclassified Title:
A STUDY OF CONSTANT ABSOLUTE VORTICITY TRAJECTORIES ON ISENTROPIC SURFACES.
Title Classification:
Unclassified
Descriptive Note:
Master's thesis,
Personal Author(s):
Carlstead, Edward Meredith
Report Date:
01 Jan 1953
Media Count:
25 Page(s)
Cost:
$7.00
Report Classification:
Unclassified
Descriptors:
(*WEATHER FORECASTING, , HIGH ALTITUDE), METEOROLOGICAL PHENOMENA, PRESSURE, VORTICES, ATMOSPHERIC TEMPERATURE, VELOCITY, WIND, CORIOLIS EFFECT, DENSITY, VECTOR ANALYSIS, UPPER ATMOSPHERE, METEOROLOGICAL CHARTS, TRAJECTORIES, SURFACES, ATMOSPHERIC MOTION
Identifiers:
CHARTS.
Abstract:
The meteorologist is ofter called upon to forecast for periods in excess of 24 hours for which simple extrapolation is generally insufficient. One method of forecasting entails preparation of prognostic surface charts and preparation of forecasts from these charts. One of the important tools used in estimating the position and intensity of surface systems is a prognostic 500 millibar chart. At present, much attention is being paid to the problem of upper air prognosis, and considerable information has been published concerning forecasting the 500 millibar surface. One aid to prognosis of upper air charts is the construction of forecast air parcel trajectories based on

the principle of conservatism of the vertical component of absolute vorticity. A fundamental equation was integrated and trajectories were obtained for particles which conserve their vertical component of absolute verticity. This trajectory is known as the Constant Vertical Component of Absolute Vorticity Trajectory.

Abstract Classification:

Unclassified

Annotation:

Study of constant absolute vorticity trajectories on isentropic surfaces.

Distribution Limitation(s):

01 - APPROVED FOR PUBLIC RELEASE

Source Code:

251450

Document Location:

DTIC

Change Authority:

ST-A USNPS LTR 1 OCT 71

[redacted]

A STUDY OF CONSTANT ABSOLUTE VORTICITY TRAJECTORIES ON ISENTROPIC SURFACES

E. [redacted]. Carlstead

A STUDY OF CONSTANT ABSOLUTE VORTICITY TRAJECTORIES ON ISENTROPIC SURFACES

by
Edward Meredith Carlstead
Lieutenant, junior grade, United States Navy

Submitted in partial fulfillment
of the requirements
for the degree of

MASTER OF SCIENCE
IN AEROLOGY

United States Naval Postgraduate School
Monterey, California
1953

This work is accepted as fulfilling
the thesis requirements for the degree of

MASTER OF SCIENCE
IN AEROLOGY

from the
United States Naval Postgraduate School

PREFACE

This paper presents the results of a study of Constant Absolute Vorticity Trajectories applied to isentropic surfaces. The objectives of this study were: first, to show that Constant Absolute Vorticity Trajectories are theoretically better applied to forecasting future positions of parcels on isentropic surfaces than on constant pressure surfaces as they are now applied; secondly, to show quantitatively the actual improvement of the trajectories on isentropic surfaces by comparing statistically results of actual forecasts from both types of charts; thirdly, to suggest how the improved technique can aid forecasting, particularily upper air prognosis.

This work was undertaken as the thesis requirement for the degree of Master of Science in Aerology at the U. S. Naval Postgraduate School, Monterey, California, during the academic year 1952-1953.

The author is indebted to Associate Professor George J. Haltiner of the Aerology Department for his very valuable assistance and constructive criticism during the investigation. He also wishes to acknowledge the assistance of Professor A. Boyd Newborn of the Mathematics Department and the author's wife, Pauline, who contributed so much help with the laborious task of decoding, computing, and entering isentropic charts.

TABLE OF CONTENTS

LIST OF ILLUSTRATIONS

TABLE OF SYMBOLS AND ABBREVIATIONS

CAV	Constant vertical component of absolute vorticity
e	Base of natural logarithms
f	The coriolis parameter
g	Acceleration of gravity
K	Temperature in the Kelvin (absolute) scale
N	Direction normal to a streamline on an isentropic map
P	Pressure
R_s	Radius of curvature of a streamline on an isentropic map
S^2	The variance of a sample of data
u	West to east horizontal component of wind velocity
v	South to north horizontal component of wind velocity
V	Wind speed
$\vec{V}$	Wind velocity
w	Vertical component of wind velocity
ζ	Vertical component of relative vorticity
ρ	Density
∇	Vector del operator

I. INTRODUCTION

The meteorologist is often called upon to forecast for periods in excess of twenty-four hours for which simple extrapolation is generally insufficient. One method of forecasting entails preparation of prognostic surface charts and preparation of forecasts from these charts. As most meteorlogists know, making accurate prognostic surface charts is easier said than done. One of the important tools used in estimating the position and intensity of surface systems is a prognostic 500 millibar chart. At present, much attention is being paid to the problem of upper air prognosis, and considerable information has been published concerning forecasting the 500 millibar surface, the most recent being Forecasting in the Middle Latitudes by Riehl and collaborators. It is hoped that this paper may shed some light on a facet of this problem and may contribute to better prognosis and forecasting.

One aid to prognosis of upper air charts is the construction of forecast air parcel trajectories based on the principle of conservatism of the vertical component of absolute vorticity, $(\zeta + f)$, where ζ is the vertical component of relative vorticity and f is the vertical component of the coriolis force known as the coriolis parameter. Rossby [8] initiated the vorticity concept by showing that under certain restrictive assumptions, the following relationship holds:

$$(\zeta + f) = \text{constant}. \tag{1}$$

The assumptions referred to above are as follows:

a. The atmosphere is barotropic.

b. The atmosphere is a homogeneous, incompressible fluid.

c. Motion is purely horizontal.

d. Friction forces are neglected.

e. There is no horizontal divergence.

Rossby [9, pp 268-289] then integrated his fundamental equation and was able to obtain trajectories for particles which conserve their vertical component of absolute vorticity. This trajectory is known as the Constant Vertical Component of Absolute Vorticity Trajectory and will be referred to as a CAV trajectory.

The assumptions necessary to derive the vorticity equation according to Rossby are obviously quite restrictive. Starr, as editor of the Journal of Meteorology (June, 1945), suggested that CAV trajectories might better be depicted on an isentropic chart than on a constant level chart as there are no solenoids on an isentropic chart. Namias [6, pp 372-374] states that from observations available isentropic surfaces appear, to the first approximation, to be substantial surfaces, i.e., surfaces that contain the same air particles from day to day. Influences of non-adiabatic nature are appreciable over long periods of time, but are usually insufficient to disrupt the fundamental isentropic flow from one day to the next. The derivation of the vorticity equation for flow on an isentropic surface requires fewer assumptions. Such restrictions as purely horizontal flow, a barotropic atmosphere, and a homogeneous

incompressible atmosphere may be removed. Now, an isentropic surface is a surface of constant potential temperature. In meteorlogical processes, potential temperature is one of the more conservative elements by which parcels of air may be identified from time to time. Since the atmosphere is normally stable, potential temperature increases with height and the atmosphere may be considered to consist of an infinite number of isentropic surfaces. Sir Napier Shaw [10, p 263] first suggested that charts of isentropic surfaces should be drawn as the motion of air is best resolved on isentropic surfaces. It will be shown in this paper that the prognostic trajectory based on the conservatism of the vertical component of absolute vorticity is theoretically and practically better suited to use on isentropic charts than on constant pressure charts as it is now applied.

II. THEORETICAL INVESTIGATION

The motion of particles on a substantial surface can be described with Lagrangian methods. The form of the vorticity equation for flow on an isentropic surface derived here using the Lagrangian method of attack is due to Haltiner*. Let x, y, z and t be normal Cartesian coordinates and let X, Y, Z and τ be Lagrangian coordinates where X and Y are coordinates of the horizontal projection of the isentropic surface, $Z = z$ and τ refers to time for the isentropic surface. Then

$$\frac{\partial p}{\partial X} = \frac{\partial p}{\partial x} + \frac{\partial p}{\partial z}\frac{\partial z}{\partial X} = \frac{\partial p}{\partial x} - g\rho\frac{\partial z}{\partial X}$$

$$\frac{\partial p}{\partial Y} = \frac{\partial p}{\partial y} + \frac{\partial p}{\partial z}\frac{\partial z}{\partial Y} = \frac{\partial p}{\partial y} - g\rho\frac{\partial z}{\partial Y}.$$

It follows from the above equations that

$$-\frac{1}{\rho}\frac{\partial p}{\partial x} = -\frac{\partial F}{\partial X} \quad \text{and} \tag{1}$$

$$-\frac{1}{\rho}\frac{\partial p}{\partial y} = -\frac{\partial F}{\partial Y} \tag{2}$$

where $F = c_p T + g z$, the stream function for an isentropic surface. In a similar way we find

$$\frac{\partial u}{\partial x} = \frac{\partial u}{\partial X} - \frac{\partial u}{\partial z}\frac{\partial z}{\partial X}, \quad \frac{\partial v}{\partial x} = \frac{\partial v}{\partial X} - \frac{\partial v}{\partial z}\frac{\partial z}{\partial X} \tag{3}$$

$$\frac{\partial u}{\partial y} = \frac{\partial u}{\partial Y} - \frac{\partial u}{\partial z}\frac{\partial z}{\partial Y}, \quad \frac{\partial v}{\partial y} = \frac{\partial v}{\partial Y} - \frac{\partial v}{\partial z}\frac{\partial z}{\partial Y}. \tag{4}$$

*Associate Professor C. J. Haltiner, U. S. Naval Postgraduate School

Further, since the motion is assumed to be isentropic,

$$w = \frac{\partial z}{\partial t} + u\frac{\partial z}{\partial X} + v\frac{\partial z}{\partial Y} . \tag{5}$$

Substituting in the equations of motion

$$\begin{aligned} \frac{\partial u}{\partial t} + u\frac{\partial u}{\partial x} + v\frac{\partial u}{\partial y} + w\frac{\partial u}{\partial z} &= -\frac{1}{\rho}\frac{\partial p}{\partial x} + fv \\ \frac{\partial v}{\partial t} + u\frac{\partial v}{\partial x} + v\frac{\partial v}{\partial y} + w\frac{\partial v}{\partial z} &= -\frac{1}{\rho}\frac{\partial p}{\partial y} - fu \end{aligned} \tag{6}$$

the expressions 1, 2, 3, 4, and 5, we obtain

$$\frac{\partial u}{\partial t} + u\frac{\partial u}{\partial X} + v\frac{\partial u}{\partial Y} = -\frac{\partial F}{\partial X} + fv \tag{7}$$

$$\frac{\partial v}{\partial t} + u\frac{\partial v}{\partial X} + v\frac{\partial v}{\partial Y} = -\frac{\partial F}{\partial Y} - fu . \tag{8}$$

Differentiating (7) with respect to Y and (8) with respect to X and subtracting, we obtain

$$\frac{\partial}{\partial t}\left[\frac{\partial u}{\partial Y} - \frac{\partial v}{\partial X}\right] + \frac{\partial u}{\partial Y}\frac{\partial u}{\partial X} + v\frac{\partial^2 u}{\partial X \partial Y} + \frac{\partial v}{\partial Y}\frac{\partial u}{\partial Y} + v\frac{\partial^2 u}{\partial Y^2} - \frac{\partial u}{\partial X}\frac{\partial v}{\partial X}$$

$$-u\frac{\partial^2 v}{\partial X^2} - v\frac{\partial^2 v}{\partial Y \partial X} - \frac{\partial v}{\partial X}\frac{\partial v}{\partial Y} = \frac{\partial f}{\partial Y}v + \frac{\partial f}{\partial X}u + f\left[\frac{\partial v}{\partial Y} - \frac{\partial u}{\partial X}\right].$$

Collecting terms

$$-\frac{\partial}{\partial t}\left[\varphi_\theta\right] + \left[\frac{\partial v}{\partial Y} + \frac{\partial u}{\partial X}\right]\left[\frac{\partial u}{\partial Y} - \frac{\partial v}{\partial X}\right] + u\frac{\partial}{\partial X}\left[\frac{\partial u}{\partial Y} - \frac{\partial v}{\partial X}\right]$$

$$+v\frac{\partial}{\partial Y}\left[\frac{\partial u}{\partial Y} - \frac{\partial v}{\partial X}\right] = u\frac{\partial f}{\partial X} + v\frac{\partial f}{\partial Y} + f\left[\frac{\partial u}{\partial X} + \frac{\partial v}{\partial Y}\right].$$

and introducing vector notation we obtain

$$-\left(\frac{\partial}{\partial \tau}[\rho_\theta] + \mathbf{V}\cdot\nabla_{2\theta}\rho_\theta\right) - \rho_\theta \nabla_{2\theta}\cdot\mathbf{V} = \mathbf{V}\cdot\nabla_{2\theta} f + f\nabla_{2\theta}\cdot\mathbf{V} + \frac{\partial f}{\partial \tau}$$

where the operator $\nabla_{2\theta} = \hat{i}\frac{\partial}{\partial X} + \hat{j}\frac{\partial}{\partial Y}$.

Finally, we may write this as

$$\frac{d}{dt}\left(\rho_\theta + f\right) + \left(\rho_\theta + f\right)\nabla_{2\theta}\cdot\mathbf{V} = 0 \qquad (9)$$

since $\tau = t$ for any particle. Now, assume the divergence term $\nabla_{2\theta}\cdot\mathbf{V} = 0$.

Then we may write the vorticity equation in the familiar form

$$\frac{d}{dt}\left(\rho_\theta + f\right) = 0 \qquad \text{or} \qquad \left(\rho_\theta + f\right) = \text{constant.} \qquad (10)$$

While this form is similar to the form derived by Rossby, there are some fundamental differences. Parcel motion is not limited to the horizontal, but is three dimensional. Moreover, a barotropic and incompressible atmosphere is not required.

III. TECHNIQUE OF INVESTIGATION

The relative vorticity may be written in a form similar to the usual expression for the vertical component of vorticity in natural coordinates

$$\zeta_\theta = \frac{V}{R_s} - \frac{\partial V}{\partial N}$$

where R_s and N are measured on the isentropic map. If we select a parcel in a broad uniform flow or in the axis of a jet stream, $\frac{\partial V}{\partial N} = 0$. Further, if the parcel is at an inflection point in the flow, $\frac{V}{R_s} = 0$. Under these conditions the CAV trajectory can be computed. It will be noted that R_s defined above is not exactly equal to the projected radius of curvature of the streamline on the isentropic surface. However, the approximation involved here is normally less than those made in the actual computation of CAV trajectories as described by Fultz [4, p 13] and revised by Wobus [12]. While approximations have to be made, it must be remembered that the true worth of a technique lies in the statistically proven results obtained.

The simplest method of obtaining a CAV trajectory is through the use of a mechanical device such as the so-called "Wiggle-Wagon" devised by Wobus [12] and currently in use in the WBAN Analysis Center, Washington, D. C. Original studies of the CAV trajectory assumed a plane earth. This assumption entailed errors due to distortion when compared to trajectories along a spherical earth. The Wobus "Wiggle-Wagon" corrects this defect. To aid meteorologists who do not have access to the "Wiggle-Wagon", the U. S. Navy

Bureau of Aeronautics Project AROWA [11] has published a table for computing CAV trajectories made from trajectories traced by the "Wiggle-Wagon". This table will be used to compute CAV trajectories in this paper. For application, it is necessary to know speed, direction, and the latitude of the parcel, all at an inflection point in the flow.

The next step in the investigation was to compute trajectories on isentropic and 500 millibar charts and test the results statistically. A rather complete compilation of upper air and surface data are available in the Northern Hemisphere Surface and 500 Millibar Charts Series published by the U. S. Weather Bureau. These remarkable publications not only have a daily series of logically analysed surface and 500 millibar charts, but also contain a compilation of all data used to plot these charts. Data were taken from the period of January-February 1949. From this data, a set of thirty isentropic charts was plotted. The 303K isentropic surface was selected because: (1) this surface was often close to the so-called "level of non-divergence" described by Bjerknes [1] ; (2) this surface often contained much of the 500 millibar wind speed maximum axis (jet); (3) the 303K isentropic surface was usually sufficiently far from the surface to remove effects of surface friction and turbulence. It was desired to select an isentropic surface containing much of the 500 millibar isotach maximum axis so computation of CAV trajectories could aid in the prognosis of the 500 millibar surface.

Inasmuch as the derivation of CAV trajectories on an isentropic surface assumes the divergence term to be zero, the selection of an isentropic surface close to the level of no horizontal divergence may be desirable. The effect of the divergence term is discussed in Chapter IV.

After the heights of the 303K isentropic surface were plotted, all available wind data pertinent to the surface were plotted. Where wind observations were available from stations other than radiosonde stations, an interpolated value of the height of the isentropic surface and the wind nearest that height were entered. Because of the fairly dense network of upper air wind observing stations in the United States, sufficiently accurate streamline analysis was possible without the time-consuming computations of stream function values.

Streamline analyses were made for 0300Z each day in the period from 6 January, 1949, to 22 January, 1949, and from 10 February, 1949, to 20 February, 1949. For each chart, a number of CAV trajectories were computed. The following conditions had to be met before choosing the initial point: (1) the point had to be in or very near an inflection point in the flow (undergoing no effects of curvature); (2) the point had to be in or near the axis of the isotach maximum (jet stream); (3) the point must be at an actual point of wind observation to obtain correct initial wind speed and direction. This procedure netted from one to four points suitable for computation of CAV trajectories per chart.

For comparison with each CAV trajectory plotted on the isentropic chart, a companion CAV trajectory was computed on the 500 millibar chart of the same time. It was not too difficult to find a companion inflection point on the 500 millibar chart as the isentropic surface was usually close to the 500 millibar surface. After the CAV trajectories were constructed on each chart, forecast wind velocities were determined by moving the parcel along the trajectory a distance equal to the initial wind speed multiplied by the number of hours to forecast time. The forecast times selected were twenty-four, forty-eight, and seventy-two hours. These forecast winds were then plotted on the verifying charts and verified. On the isentropic chart, verification depended on the forecast position falling within the observational network. If the forecast position fell within the network, but not on a particular station, the forecast winds were verified by linear interpolation between nearby stations. However, care was taken to use only stations where linear interpolation would be reasonable. On the 500 millibar chart, forecast winds were verified in a similar manner if the forecast position fell within the observational network or on a reporting station. If the forecast position on the 500 millibar chart fell on neither of these places, then contours were assumed to be streamlines, and gradient winds were measured to verify. Since verification on isentropic charts depended on forecast positions falling in the North American network or on a particular station, the number of possible

verifications fell off drastically after forty-eight hours. However, with hemispherical 500 millibar charts available, forecasts made on the 500 millibar chart could always be verified. All 500 millibar CAV trajectories were carried out to seventy-two hours.

In verifying forecast winds, observed wind direction error was arbitrarily selected negative if the observed wind direction was to the right (clockwise) of the forecast wind direction and positive if the observed wind direction was to the left (counter-clockwise) of the forecast wind direction. Similarily, wind speed error was selected negative if observed wind speed was less than forecast and positive if the wind speed was greater than forecast. All forecast winds and verifications were tabulated in a form suitable for statistical testing.

Histograms of wind speed error and wind direction error were prepared for twenty-four and forty-eight hour forecast times for both the isentropic and 500 millibar charts. These histograms are depicted as Figures 1 through 4. Wind speed errors were grouped into cells each having a cell interval of 10 knots error. The cell midpoints are for $\pm 0, \pm 10, \pm 20$ etc., knots error. Since the cell boundaries are exactly halfway between the cell midpoints, some of the observations fell on the cell boundaries. In this case, it was deemed best to divide such observations between each adjacent cell. Less trouble was encountered in grouping wind direction error. All wind direction errors were in increments of 10 degrees and values of $0, \pm 10$ ± 20, etc. degrees of error were taken as cell midpoints.

After the data were grouped in histograms, normal curves were fitted in accordance with the method described by Hoel [5, pp 191-194]. After obtaining these fitted normal curves, χ^2 tests were performed to determine if each sample of data could reasonably be from a normal population. In all cases the sample distributions could reasonably be said to be from normal populations, although in two cases the value of χ^2 was close to the critical value. Restrictions on the χ^2 test were met by grouping cells with too few frequencies together. After showing normality of the data, the distributions of data from the isentropic charts were compared to similar distributions from the 500 millibar charts by the use of the "F" test. The "F" test was made to determine if compared data distributions from the isentropic and 500 millibar charts could statistically be from the same parent normal population. The purpose here is to show that a given distribution of data from the isentropic charts is not from the same normal population as the similar data distribution from the 500 millibar charts. If there is a significant difference, then inspection and intuition will reveal which of the two types of charts are better suited to forecasting by means of CAV trajectories.

IV. RESULTS

It is well to look first at the data in "everyday" terms to find what kind of results a forecaster may expect. If it is arbitrarily decided that a wind direction forecast will verify as a "hit" if it is within 20 degrees of observed direction, then we find that 96.4% of the twenty-four hour wind direction forecasts from CAV trajectories on isentropic charts verified as "hits". By comparison, 76.3% of similar forecasts from 500 millibar charts verified as "hits". With forty-eight hour wind direction forecasts, 81% from isentropic charts verified as "hits" and 41% from 500 millibar charts.

If it is arbitrarily decided that 15 knots of wind speed error is not too much to verify as a "hit", we find that 76% of twenty-four hour wind speed forecasts from trajectories on isentropic charts verified as "hits". Of the data from the 500 millibar charts, 42.4% of twenty-four hour wind speed forecasts verified as "hits". Similarly, forty-eight hour wind speed forecasts verified 78.5% from isentropic chart data and 39% from 500 millibar chart data. So, percentagewise, forecasting wind vectors by CAV trajectories on isentropic charts was superior to forecasting wind vectors by CAV trajectories on 500 millibar charts during the period of this study.

Figures 1 through 4 are histograms of error between observed and forecast wind speed and direction. Applying standard statistical methods, normal curves were fitted to the data. The χ^2 test was applied to determine if the distributions of error were likely to be from a normal population. Only the twenty-four and forty-eight hour

errors were compared and tested as the seventy-two hour isentropic sample was too small. In each case tested, the distribution was shown to be reasonably from a normal population. In cases of data from isentropic charts, there was little doubt that the distributions were from normal populations. But in cases from the 500 millibar charts, the values of χ^2 were close to the critical values and, therefore, there is some doubt that they may be from a normal population. However, since the values of χ^2 did fall below the critical values, we will treat such data as being from normal populations.

The "F" test [5, pp 152-154] is a statistical test for comparing variances (s^2) of two samples of data to determine if the two samples can reasonably be from the same normal population. The basic requirement of the "F" test is that the data samples must each be from normal populations, although not necessarily the same normal population. This is why it was necessary to show normality of the data samples above. To apply the "F" test, we first postulate that there is no significant difference between samples tested, i.e., $s_1^2 = s_2^2$. This is the null hypothesis. If the value of F computed falls below a critical value, the null hypothesis is not denied and there is no statistical difference between the two samples. If the value of F computed is higher than the critical value, the null hypothesis is denied, and there is a statistically significant difference between the two samples and they are not reasonably from the same parent normal population. It is this last condition we wish to obtain here. The results of applying the "F" test are as follows:

1. Twenty-four Hour Wind Direction Error. The variance of data from the isentropic charts $s_1^2 = 1.24$. The variance of data from the 500 millibar charts $s_2^2 = 6.37$. Then

$$F = s_2^2 / s_1^2 = 5.14.$$

F_c at a 95% level of belief is 4.90. Therefore, the samples tested are significantly different and the null hypothesis is denied.

2. Forty-eight Hour Wind Direction Error. The variance of date from the isentropic charts $s_1^2 = 3.15$. The variance of data from the 500 millibar charts $s_2^2 = 30.72$. Then

$$F = s_2^2 / s_1^2 = 9.75.$$

F_c at a 95% level of belief is 3.75. This is highly significant and the null hypothesis is certainly denied.

3. Twenty-four Hour Wind Speed Error. The variance of data from the isentropic charts is 155.7. The variance of data from the 500 millibar charts is 413.1. Then

$$F = 2.65.$$

F_c at a 95% level of belief is 5.19 and, therefore, the null hypothesis is not denied and there is no significant difference between the samples of data.

4. Forty-eight Hour Wind Speed Error. The variance of data from the isentropic charts is 127.3. The variance of data from the 500 millibar charts is 515.5. Then

$$F = 4.05.$$

At a 90% level of belief the value of $F_c = 4.00$, and at this level the difference between the samples becomes significant.

Significant results were obtained in the cases of wind direction error and in one case of wind speed error. In each of the cases where significance was obtained, an intuitive examination of the data shows that it is the data from trajectories constructed on isentropic charts that are better.

It is gratifying to note that the greatest improvement was shown for wind direction forecasting for a forty-eight hour period. In much operational forecasting, wind direction is usually deemed more important than wind speed for prognostic work. The proper placing of troughs and ridges and associated weather patterns depends greatly on correct wind direction forecasts. Therefore, from the results obtained, the CAV trajectory method will show greatest improvement over the present system of taking CAV trajectories on constant pressure charts if used on isentropic charts to forecast wind direction, at least up to forty-eight hours.

A recent study of CAV trajectories along a psuedo-600 millibar chart was published by Bruch [2]. Bruch's results on wind direction error are quite similar to results obtained herein for the 500 millibar chart. Bruch did not verify wind speeds.

It is realized that the isentropic chart leaves much to be desired as an operational weather chart. At present the chart is of course laborious to plot since no isentropic data are transmitted on teletype circuits; however, if such data were transmitted on teletype circuits, streamline analysis would take little longer to prepare than the present 500 millibar chart. Another difficulty is that the

movement of the isentropic surface is not easy to predict. Since the CAV trajectory developed herein is a two dimensional projection of a three dimensional path, the height of the parcel in the future is in doubt. Of course, if the isentropic surface did not move, the future position of a parcel would be certain. But, this is not generally the case. A future study to correlate this study with the prognosis of isentropic surfaces could be to advantage. Nonetheless, the computation of CAV trajectories on an isentropic surface can be of value to prognosis of a nearby constant pressure surface. The positions of prognostic troughs and ridges of the isentropic flow can be placed on a nearby constant pressure surface.

From study of the CAV trajectories on the isentropic charts of this paper, it qualitatively appears that parcels imbedded in northwesterly flow descend as they move southeastward, whereas parcels imbedded in southwesterly flow rise as they move northeastward.

In the final form of the vorticity equation there is a divergence term that is assumed to be zero. This assumption is not always fulfilled in the atmosphere. The effect of this divergence term may be important. For illustration, let the divergence term $\nabla_{2\theta} \cdot V$ be constant in equation (9) and integrating with respect to t, we obtain

$$\left(\rho_\theta + f\right) = c e^{-(\nabla_{2\theta} \cdot V)\Delta t} .$$

Let $t=0$ at the initial inflection point, where also $\zeta_\theta=0$. Then

$$(\zeta_\theta+f)=c=f_o$$

and

$$\zeta_\theta = f_o\, e^{-(\nabla_{z\theta}\cdot V)\Delta t} - f. \qquad (11)$$

As can be seen, positive values of the divergence term in a northwesterly flow will cause a negative contribution to relative vorticity of a parcel causing it to go farther south than under a CAV trajectory. Positive values of the term in southwesterly flow will have a similar effect on the relative vorticity of a parcel causing it to not reach the maximum latitude indicated by a CAV trajectory. Negative values of the divergence term will cause positive contributions to the relative vorticity of a parcel. In northwesterly flow this will cause a parcel to curve more cyclonically than would be indicated by a CAV trajectory and to curve less cyclonically in southwesterly flow. Fultz [4, pp 32-109] mentions that in a lower level (10,000 foot level) the average type of deviation from CAV trajectories is such that could be caused by horizontal velocity divergence in northwesterly flow and convergence in southwesterly flow. Now,

$$\nabla_{z\theta}\cdot V = \frac{\partial u}{\partial X}+\frac{\partial v}{\partial Y} = \left(\frac{\partial u}{\partial x}+\frac{\partial v}{\partial y}\right)+\left(\frac{\partial u}{\partial z}\frac{\partial z}{\partial X}+\frac{\partial v}{\partial z}\frac{\partial z}{\partial Y}\right).$$

Thus, the divergence term is composed of two parts, horizontal velocity divergence and a shear term. Fleagle [3] and Panofsky [7]

have given several values for horizontal velocity divergence, with a range of about $\pm$ 5 x 10^{-6} per second. The values of the shear term could be computed at initial inflection points for thirty-four of the CAV trajectories on isentropic charts of this study. In fourteen cases the term was less than 10^{-7} per second. In eleven cases the value of the shear term was approximately 10^{-6}, and in nine cases, approximately -10^{-6} per second. Usually, the shear term was positive or negative if the flow was up or down the isentropic surface respectively. From this we see that in about 60% of the cases studied, the shear term was of the same order of magnitude as the horizontal velocity divergence. In these cases the shear term either canceled or doubled the horizontal velocity divergence term. Now, if the assumption of $\nabla_{2\theta} \cdot \mathbf{V} = 0$ were the most important assumption in the development of CAV trajectories, we might expect forecasting of future positions of parcels by CAV trajectories on isentropic surfaces to give, in some cases, greater error than from applying CAV trajectories to constant pressure surfaces. This was not observed in the data collected in this study. This may suggest that the assumption of no horizontal divergence is not too restrictive, and that possibly one of the other assumptions made by Rossby is more restrictive, e.g., assumption of purely horizontal motion.

If we take a large constant value for horizontal velocity divergence, say 6 x 10^{-6} per second, take a like value for the

shear term, assume a time period of twelve hours, and use these values in equation (11), we would find that the value of f_o at, say, 45° is reduced by 33⅓ or to the value of f at latitude 33°. But, this is an extreme case, and the effects of the divergence term are usually much less. However, since the assumption of $\nabla_{2\theta} \cdot V = 0$ does lead to error, it seems that some future research could be profitably spent introducing quantitative values for the divergence term and computation of a trajectory incorporating this correction to the CAV trajectory for use in more accurate forecasting.

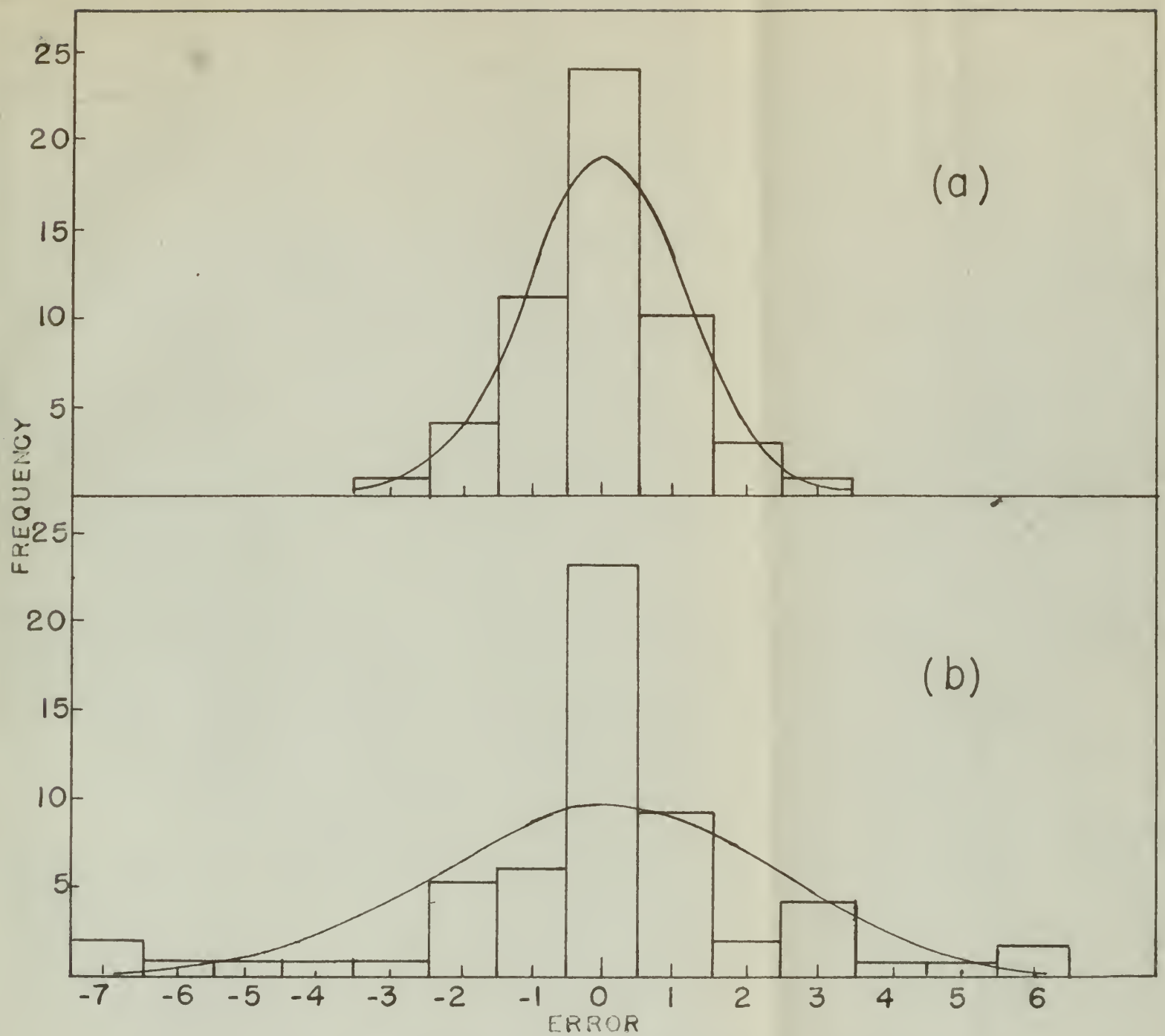

Distribution of twenty-four hour wind direction error from (a) isentropic charts and (b) from 500 millibar charts
Error: tens of degrees

Figure 1.

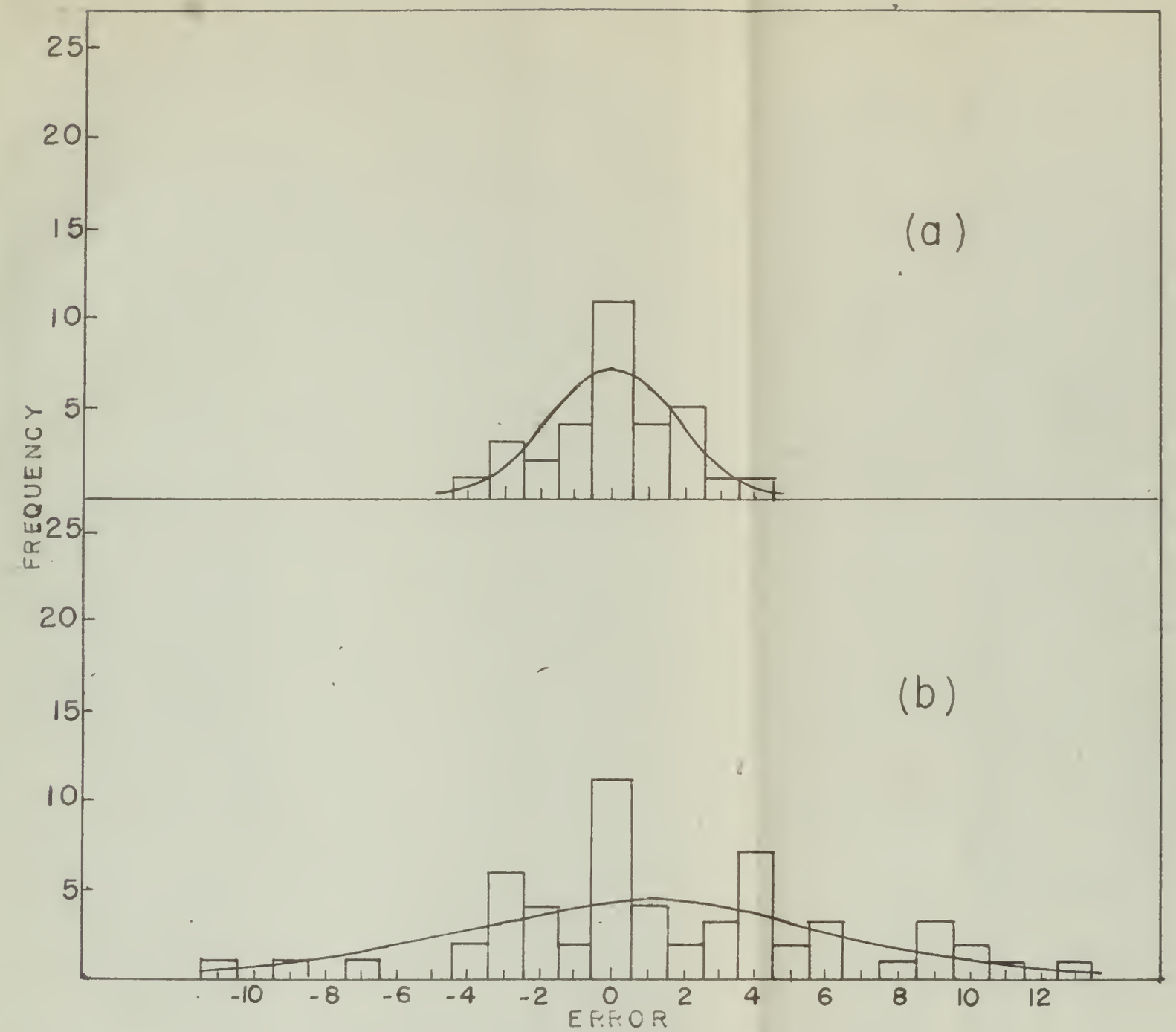

Distribution of forty-eight hour wind direction error from (a) isentropic charts and (b) from 500 millibar charts
Error: tens of degrees

Figure 2.

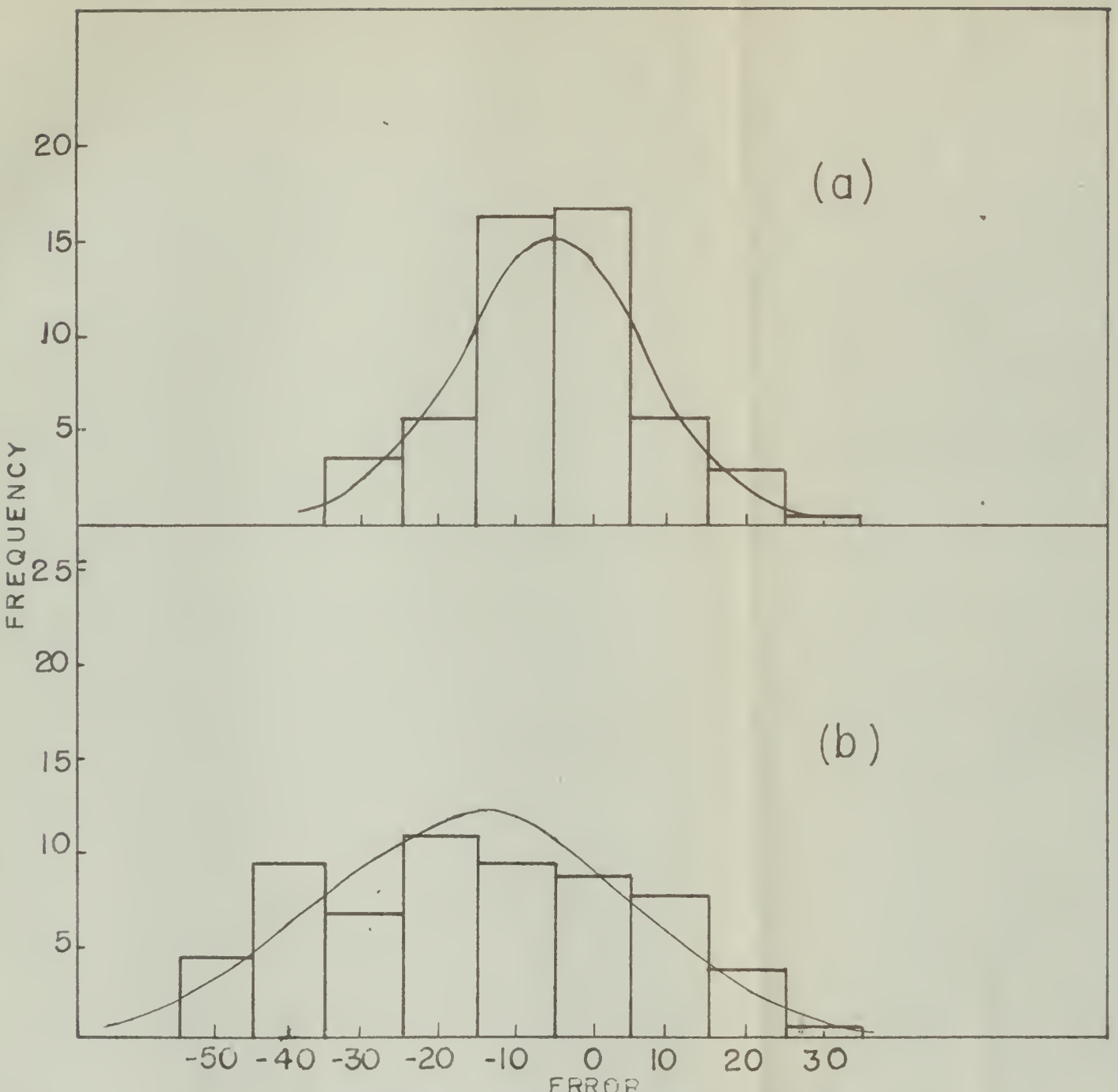

Distribution of twenty-four hour wind speed error from (a) isentropic charts and (b) from 500 millibar charts
Error: knots

Figure 3.

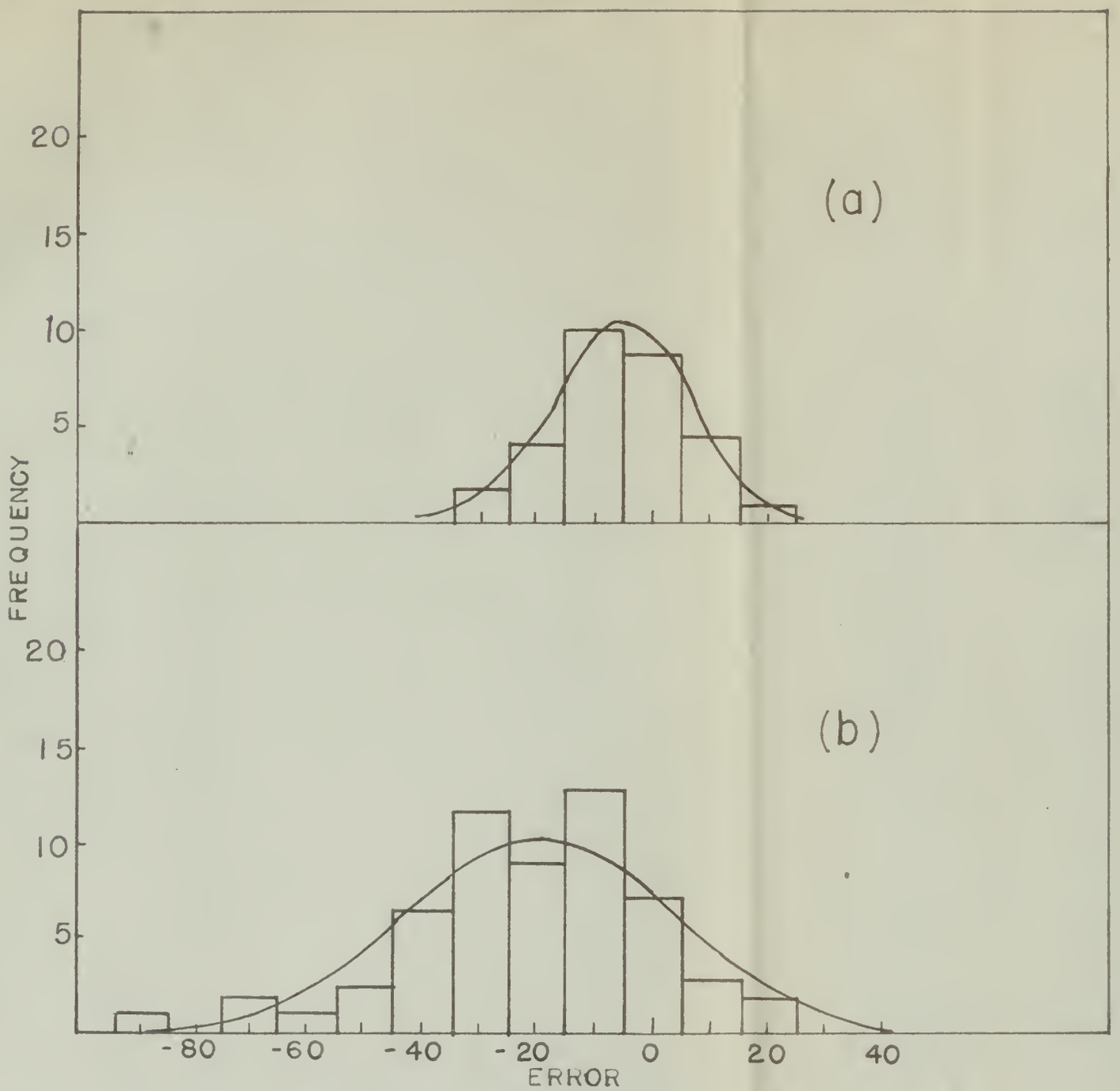

Distribution of forty-eight hour wind speed error from (a) isentropic charts and (b) from 500 millibar charts
Error: knots

Figure 4.

BIBLIOGRAPHY

1. Bjerknes, J., and Holmboe, J. On theory of cyclones. Journal of Meteorology, 1:1-22. September 1944.

2. Bruch, A. Verification of constant absolute vorticity trajectories. Experiments in quantitative prediction with the aid of upper air charts. Chicago, Department of Meteorology of the University of Chicago, October 1952.

3. Fleagle, R. Quantitative analysis of factors influencing pressure changes. Journal of Meteorology, 5:280-295. December 1948.

4. Fultz, D. Upper air trajectories and weather forecasting. Miscellaneous Report No. 19, Chicago, University of Chicago Press, 1944.

5. Hoel, P. Introduction to mathematical statistics. New York, Wiley and Son, 1947.

6. Namias, J. Isentropic analysis (Petterssen, Weather analysis and forecasting). New York, McGraw-Hill, 1940.

7. Panofsky, H. Objective weather map analysis. Journal of Meteorology, 6:381-395, December 1949.

8. Rossby, C. G. Variations in intensity of zonal circulation of the atmosphere and displacement of the semi-permanent centers of action. Journal of Marine Research, 2:38-55, June 1939.

9. _____ Forecasting of flow patterns in the free atmosphere by a trajectory method (Starr, Basic principles of weather forecasting). New York, Harper and Brothers, 1942.

10. Shaw, Sir Napier. Manual of meteorology, Vol. III. Cambridge, Cambridge University Press, 1933.

11. U. S. Navy Bureau of Aeronautics Project AROWA. Topical outline of refresher course for reserve aerologists in recent developments in upper air analysis and forecasting. Norfolk, Section 7, 1952.

12. Wobus, H. B. A constant vorticity trajectory differential analyser. Unpublished, 1950.